

Research Article

The Roles of Alkyl Branches of Ionic Liquid in the Corrosion Resistance of Pb/Sb/Sn Grids Alloy in Lead-Acid Battery

Behzad Rezaei, Ali Asghar Ensafi, and Ahmad Reza Taghipour Jahromi

Department of Chemistry, Isfahan University of Technology, Isfahan 8415683111, Iran

Correspondence should be addressed to Behzad Rezaei, rezaei@cc.iut.ac.ir

Received 23 March 2011; Revised 15 May 2011; Accepted 16 May 2011

Academic Editor: Abel César Chialvo

Copyright © 2011 Behzad Rezaei et al. This is an open access article distributed under the Creative Commons Attribution License, which permits unrestricted use, distribution, and reproduction in any medium, provided the original work is properly cited.

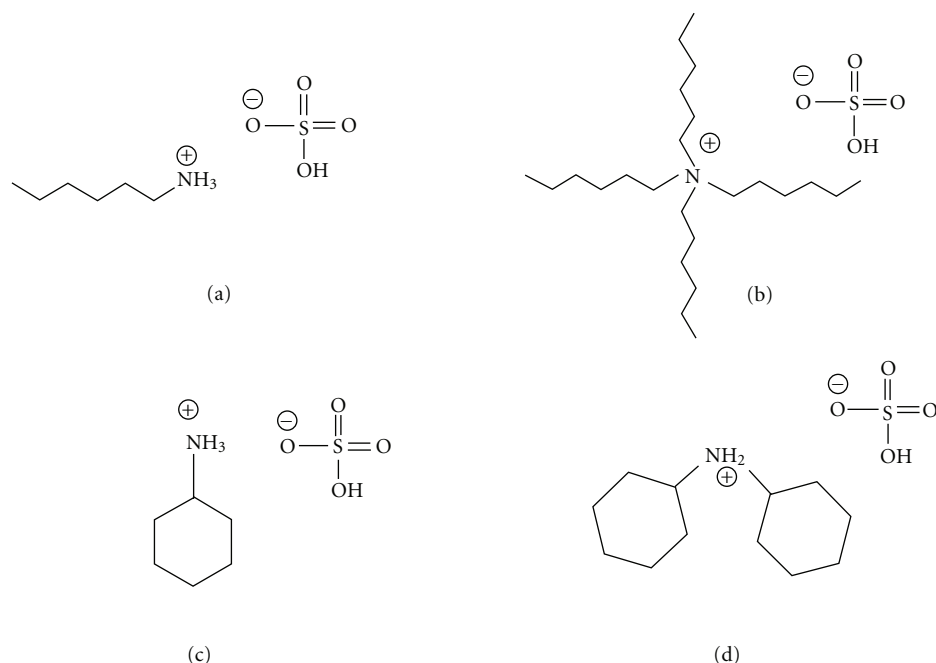
This paper describes the effects of ionic liquids (ILs) including mono, bicyclohexyl, and tetrahexyl ammonium hydrogen sulphate on the corrosion behaviour of Pb/Sb/Sn grids alloy of lead-acid battery with Pb, Sb (1.66 wt%), and Sn (0.24 wt%). Electrochemical behaviour has been investigated using Tafel plots and electrochemical impedance spectroscopy with various concentrations of ILs as electrolyte additives in 4.0 mol·L⁻¹ sulphuric acid. The obtained results indicated that, by increasing number of alkyl or cycloalkyl branches in ILs, the corrosion rate of the lead alloy decreases, whereas inhibition efficiency shows a reverse effect. In the presence of all ILs in different concentrations, conversion current of PbSO₄ to PbO₂ (i_a and i_c) increases, while the reversibility, deduced from peak potential differences, decreases. Also, the effect of ILs adsorption model on the corrosion behaviour of electrode was proposed.

1. Introduction

Lead-acid batteries as electrical power source are used in different applications such as vehicles, submarines, and emergency systems. It is still widely used as a starter source in the automotive field, although there have been a growing number of other applications. Its advantages are low cost, high voltage per cell, and good capacity life [1]. However, some disadvantages can be observed such as water loss, the need to increase specific energy and to extend deep cycle life. The improvement of the life time may essentially depend on the grid materials. Pb-Sn, Pb-Sb and Pb-Ca-Sn alloys are commonly used in the production of positive and negative grids, connectors, posts, and straps components of both valve regulated lead acid (VRLA) and starting, lighting, and ignition (SLI) batteries which are widely applied in automotive and telecommunication services [2, 3]. Increasing of Sb concentration in the Pb-Sn alloy led to decreases in hydrogen overpotential and improvement of the alloy casting, therefore 1–3.5 percent of Sb is added to produce lead alloy for battery manufacturing. Water loss is an aging factor that cannot be compensated by refilling. Water loss occurs, even when a perfect internal oxygen cycle is established, because of the unavoidable secondary reactions that provide hydrogen evo-

lution and grid corrosion. This problem is decreased by using some additive material in lead-acid batteries, such as ILs [4, 5]. Therefore one of the important issues is surveying the effect of additive material on the corrosion of this type of batteries.

In the recent two decades, the study of the corrosion in lead-acid batteries or lead alloy batteries has increased, because grid corrosion is a key determinant of the functional properties and life of lead-acid batteries. Some of the studies have been done on the effect of sulphuric acid concentration and the corrosion of lead at constant potential or under certain service conditions [6–12]. Boctor et al. have studied the evaluation of the corrosion of lead alloys and developed a mathematical model for lead-acid batteries for tropical applications by an electrometric method [7]. Also Slavkov et al. have studied the effect of Ca and Sn on corrosion of these batteries and have showed that doping of Pb with Sn and Ca is seen to improve the reversibility and charging efficiency of lead anodes that were used in lead-acid batteries. However, one drawback of these materials is their increased corrosion rate as compared to pure lead anodes [12]. Hence, other authors studied the corrosion behaviour of lead alloy [13–15] and used different organic compounds containing nitrogen, oxygen, and/or sulfur [16–22] and amino acids as inhibitors



SCHEME 1: Molecular structure of (a) hexyl ammonium hydrogen sulphate, (b) tetrahexyl ammonium hydrogen sulphate, (c) cyclohexyl ammonium hydrogen sulphate, (d) bicyclohexyl ammonium hydrogen sulphate.

on the corrosion of Pb/Ca/Sn alloy [23]. A literature survey shows that most of the organic inhibitors will act upon adsorption on the metal surface. The adsorption of inhibitors takes place through heteroatoms such as nitrogen, oxygen, phosphorus, and sulfur, triple bonds, or aromatic rings. The inhibitors effect is increased in the order $O < N < S < P$ [21]. Nowadays, the application of ionic liquids for improving characterization of lead-acid batteries is an important issue. In this work we have studied the effect of four different alkyl and cycloalkyl ammonium hydrogen sulphate (Scheme 1) on the corrosion of lead-antimony alloy in sulphuric acid electrolyte.

2. Experimental

2.1. Chemicals. All voltammetric experiments were performed using SAMA-500 Electroanalyzer system (Isfahan, Iran) connected to a personal computer. Electrochemical impedance spectroscopic (EIS) measurements were performed by employing an Autolab PGSTAT-12, and obtained results were fitted and analyzed using FRA4.9 software. For all experiments, a conventional three-electrode system was used which consisted of a working electrode (Pb-Sb-Sn alloy), a platinum counterelectrode, and a saturated calomel electrode (SCE) as a reference electrode (the SCE electrode is used in lead-acid system studies, but it is not used (all the time; see [12])).

2.2. Materials and Reagents. Analytical reagent grade chemicals and doubly distilled water were used in preparation of all solutions. The electrolyte was $4.0 \text{ mol} \cdot \text{L}^{-1}$ sulphuric

acid which was prepared from concentrated H_2SO_4 (98%, Merck) and doubly distilled water. Pavlov et al. studied influence of H_2SO_4 concentration on the behaviour of lead-acid batteries, and the clear distinction between the two types of LAB implies that, most probably, it is the high H_2SO_4 concentration in VRLAB that limits the cycle life performance of these batteries [22]. Besides, in the most type of lead-acid batteries (such as SLI and UPS) H_2SO_4 concentration is about 4 M. Therefore, in this study sulphuric acid concentration of 4 M was selected.

Ionic liquids hexyl ammonium hydrogen sulphate (HAHS), monocyclo ammonium hydrogen sulphate (MCHAHS), and bicyclohexyl ammonium hydrogen sulphate (BCHAHS) employed in this study were synthesized and purified in our laboratory by using the recommended method in [23], and tetrahexyl ammonium hydrogen sulphate (THAHS) was purchased from Sigma-Aldrich (Switzerland). Ionic liquids solutions (5.0 , 10.0 , 15.0 , and $20.0 \mu\text{g mL}^{-1}$) were prepared by adding an appropriate amount of ILs to $4.0 \text{ mol} \cdot \text{L}^{-1}$ sulphuric acid.

2.3. Preparation of the Working Electrodes. The iron mold with cooling system and temperature control unit as the same as grid casting machine of Sovema Co. (Verona, Italy) was used for preparing the working electrode. Antimony from the positive grid can migrate through the electrolyte and be deposited on the surface of the negative plate, where it lowers the overpotential for hydrogen evolution [24]. This leads to lower charge voltage, increased self-discharge, and therefore, increased water loss of the battery. To avoid such harmful effects of antimony, the grids were made with low

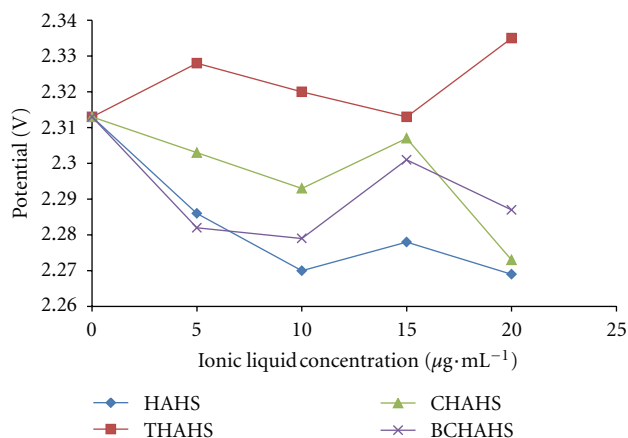


FIGURE 1: Oxygen oxidation potential by scan rate 50.0 mV s^{-1} in $4.0 \text{ mol dm}^{-3} \text{ H}_2\text{SO}_4$ in various concentrations of ILs at the current density in 4.0 mA cm^{-2} at the anodic scan.

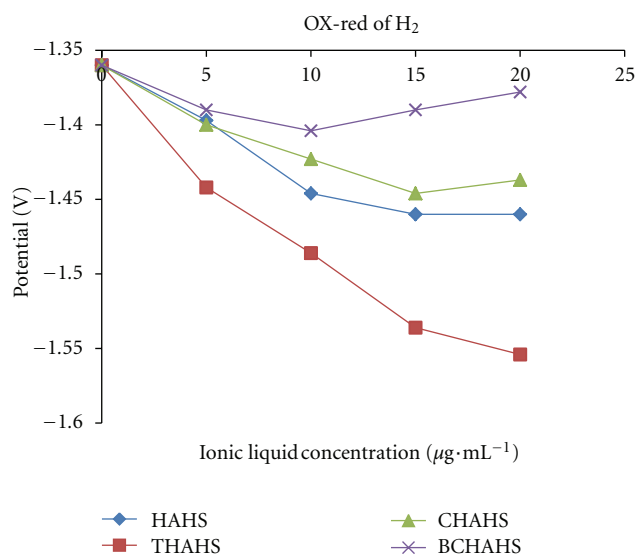


FIGURE 2: Effect of different ILs and their concentrations on the hydrogen evolution overpotential of Pb-1.6% Sb-Sn alloy in $4.0 \text{ mol dm}^{-3} \text{ H}_2\text{SO}_4$, scan rate 50.0 mV s^{-1} , and current density of 8.0 mA cm^{-2} for the cathodic scan.

antimony alloy (1-2 wt.%) in maintenance-free batteries. Therefore, in this study due to the presence of antimony in the electrode, most experiments were carried out on Pb—1.6% Sb alloy. The working electrode, a wire with geometric area of 1.0 cm^2 with Pb-1.66 wt% Sb, 0.24 wt% Sn composition, was prepared and its surroundings were enveloped with an epoxy resin.

2.4. Procedure. In order to remove any oxides and sulphates formed on the surface of the electrode, prior to each experiment, the lead alloy electrode was mechanically polished with water-resistant emery paper (P1000) throughout being rinsed with doubly distilled water. Cyclic voltammograms of lead alloy electrodes in sulphuric acid solution with and without IL in the potential region between hydrogen and

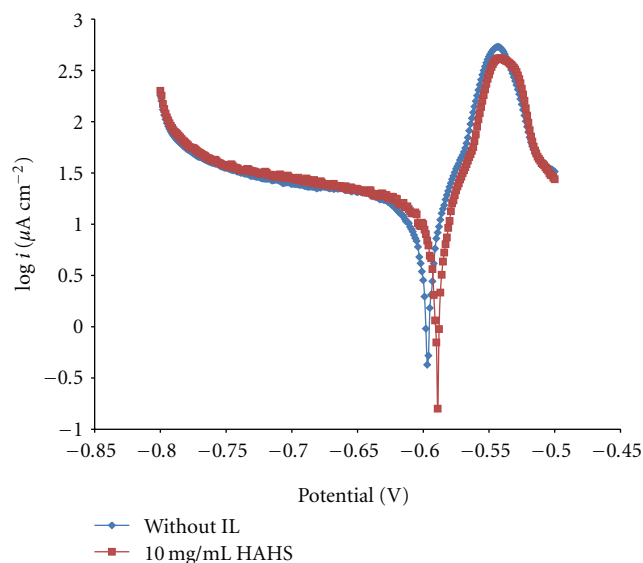


FIGURE 3: Experimental potentiodynamic polarization curves in the absence and presence of HAHS in $4.0 \text{ mol L}^{-1} \text{ H}_2\text{SO}_4$ at Pb-Sb-Sn alloy. Conditions: Immersion time, 5 min; Scan rate, 5 mV s^{-1} .

oxygen evolution (-2.50 to $+2.50 \text{ V}$ versus SCE) were obtained at a sweep rate of 50.0 mV s^{-1} . For evaluation of the effects of these ILs on the corrosion rate of the alloy, linear sweep voltammogram (LSV) and Tafel polarization measurement were carried out at a scan rate of 5.0 mV s^{-1} from -200.0 to $+200.0 \text{ mV}$ related to the open circuit potential. This mentioned potentiodynamic range is corresponding to -800.0 and -300.0 mV versus SCE. EIS measurements were carried out after 300 s of exposure of the lead alloy in the solution to reach a steady-state condition. The frequency range was set from 10^5 Hz to 10^{-1} Hz with potential amplitude of 10.0 mV in open circuit potential. Micrographs of lead alloy electrodes after one cycle of charge and discharge were obtained with Philips-XL30 (Eindhoven, The Netherlands) scanning electron microscope. Before taking scanning electron microscopy (SEM) imaging, a thin layer of gold was deposited on the electrode because epoxy resin is electrical insulator. All experiments were carried out at room temperature (298 K).

3. Result and Discussion

3.1. Oxygen and Hydrogen Evolution Overpotential. Oxygen oxidation potential by scan rate 50.0 mV s^{-1} in $4.0 \text{ mol dm}^{-3} \text{ H}_2\text{SO}_4$ in various concentrations of ILs at the anodic scan is shown in Figure 1. The obtained results show that with increasing the number of linear alkyl branches in alkylammonium cation, oxygen oxidation overpotential increases, while the increase in the number of cycloalkyl branches in cycloalkyl ammonium cation decreases the oxygen oxidation overpotential.

Figure 2 shows the effect of different ILs and their concentrations on the hydrogen evolution overpotential. In the presence of all four ionic liquids, hydrogen evolution potential shifts to more negative values. Among them, THAHS

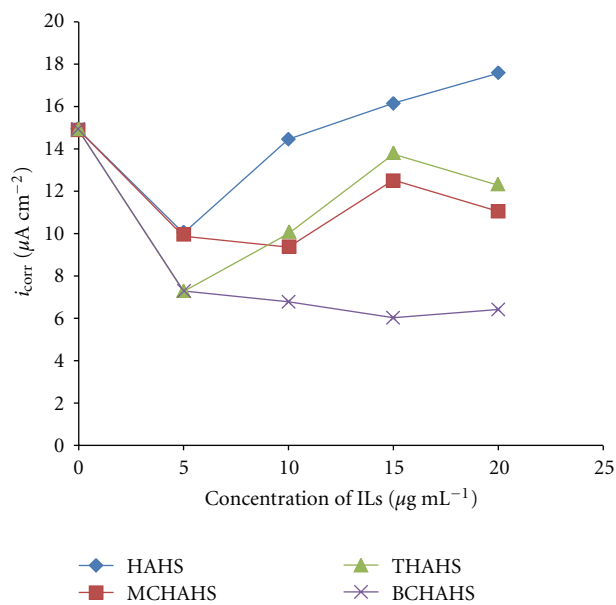


FIGURE 4: Corrosion current of Pb-Sb-Sn electrode in various ILs concentration is in $4.0 \text{ mol} \cdot \text{L}^{-1} \text{ H}_2\text{SO}_4$. Conditions: scan rate, 5 mV s^{-1} ; immersion time, 5 min.

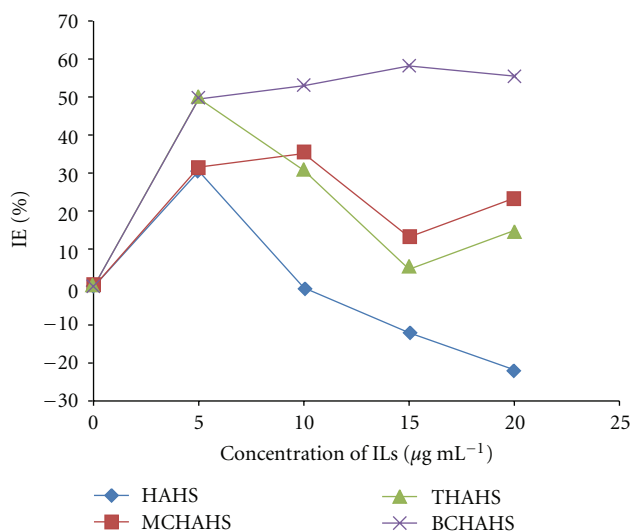


FIGURE 5: Inhibition efficiency from polarization measurements in various concentrations of ILs. Conditions: scan rate, 5 mV s^{-1} ; H_2SO_4 $4.0 \text{ mol} \cdot \text{L}^{-1}$; immersion time, 5 min.

has the most significant effect on the hydrogen overpotential. Also, Figure 2 illustrates that, with increasing the number of alkyl branches in alkylammonium cation, hydrogen overpotential has become more negative but with increasing the number of cycloalkyl branches in cycloalkyl ammonium cation, hydrogen overpotential has become more positive. The important point, which is obtained from the results, is that increasing in hydrogen overpotential has a linear correlation with the number of alkyl chain in alkylammonium cations, that is, tetra-HAHS with long alkyl groups is the most effective ionic liquid which can considerably impede the hydrogen gas evolution and hence, water lose.

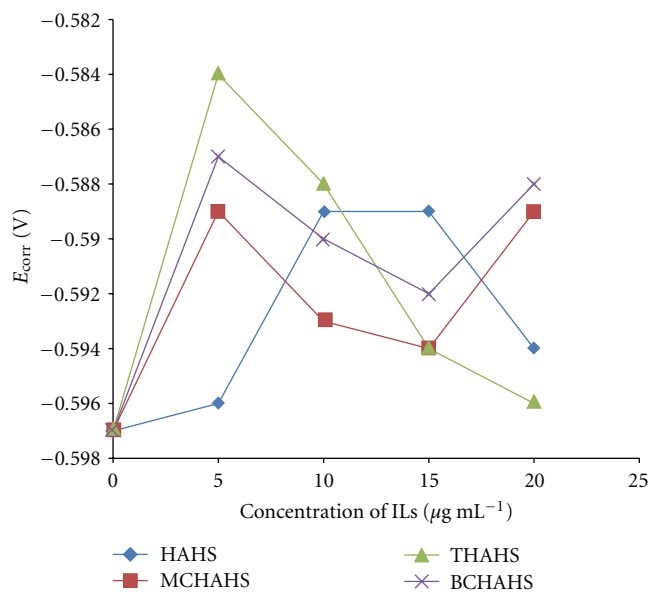


FIGURE 6: Effect of different ILs and their concentrations on the corrosion potential of Pb-Sb-Sn alloy. Conditions: Scan rate, 5.0 mV s^{-1} ; H_2SO_4 $4.0 \text{ mol} \cdot \text{L}^{-1}$; Immersion time, 5 min.

3.2. Grid Corrosion Studies. In principle, corrosion of lead starts at equilibrium potential of the cathode electrode. It is important to note that the corrosion behaviour analysis of the present work is different from the studies of PbO/PbO_2 formation which occurs at much higher potentials [25, 26]. At the open circuit potential, because no current flows through the electrode thus, discharge reaction and hydrogen evolution should balance each other. The result of this balance is the corrosion potential (E_{corr}) in which no external current (i_{corr}) appears. The effect of the presence of ionic liquids on the electrochemical corrosion behaviour of Pb-1.6% Sb -Sn electrode in sulphuric acid solution was investigated using electrochemical impedance spectroscopy (EIS) and potentiodynamic polarization tests. Figure 3 shows the Tafel plot, in which E_{corr} and i_{corr} were obtained by extrapolation of linear parts of the cathodic and anodic branches. The corrosion rate (C.R.) was calculated using the following:

$$\text{C.R. [meter per year (mpy)]} = 207.6 \left(\frac{ai_{\text{corr}}}{nD} \right), \quad (1)$$

where a is atomic weight of alloy (g mol^{-1}), D is density of alloy (g cm^{-3}), and n is the number of electrons participated in corrosion reaction [4] (for this alloy $a = 204.498 \text{ g} \cdot \text{mol}^{-1}$, $D = 11.27 \text{ g} \cdot \text{cm}^{-3}$ and $n = 2$); $\text{IE}\% = (1 - (i_{\text{corr}}/i_{\text{corr}}^0)) \times 100$ was used to calculate inhibition efficiency (IE) from the polarization measurements, where i_{corr} and i_{corr}^0 are the corrosion current densities in the presence and absence of IL in solutions, respectively. The results of the corrosion parameters which are given in Table 1 clearly indicate that i_{corr} and corrosion rate of the lead alloy decreased with increasing in the number of branches of alkyl and cycloalkyl ILs. Figure 4 shows a relation between i_{corr} and concentration of ILs. The results showed that IE% increased by increasing the number of alkyl and cycloalkyl branches of ILs (Figure 5). Figure 6

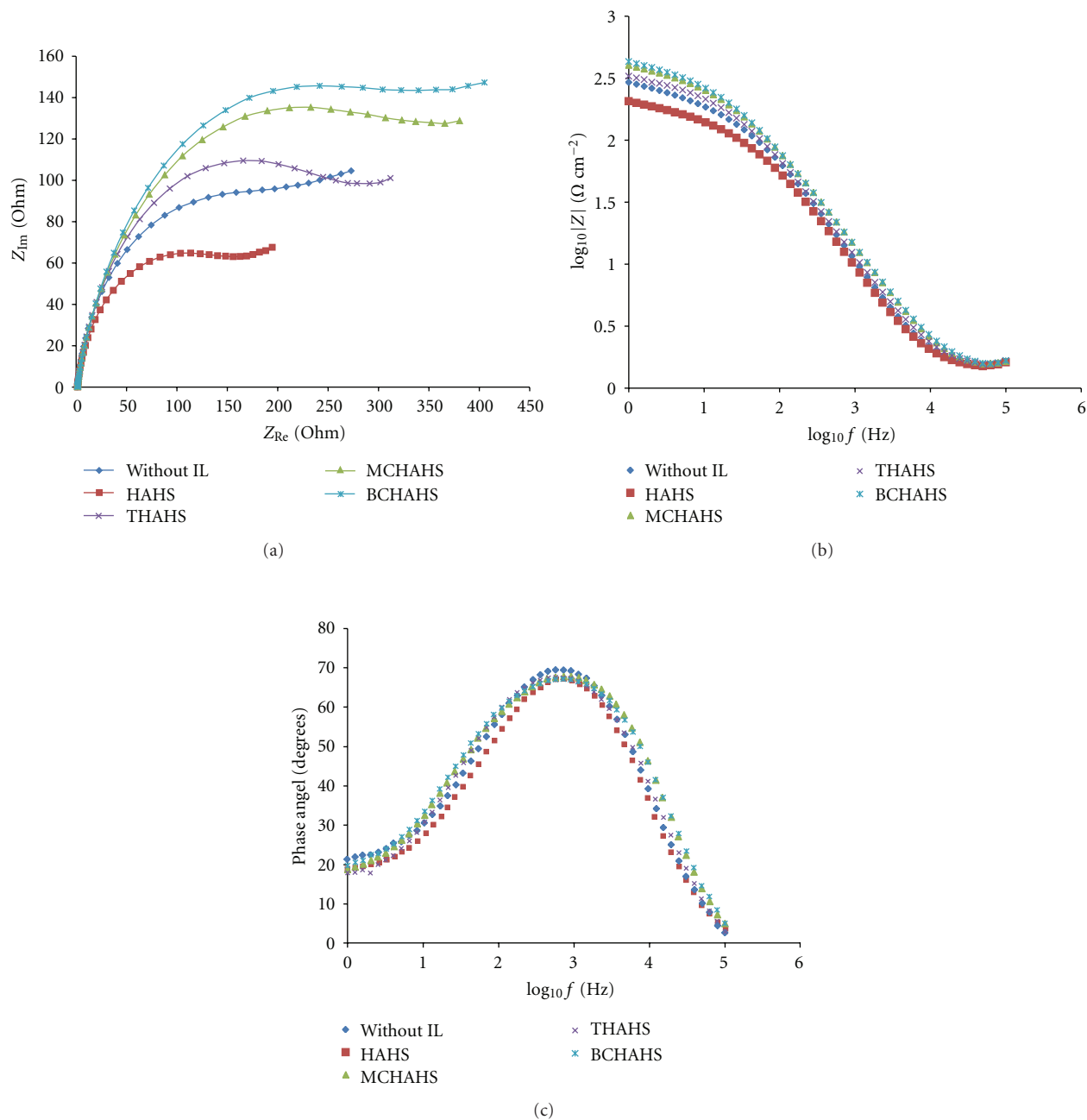


FIGURE 7: Nyquist (a) and Bode diagrams (b and c) of Pb-Sb-Sn alloy in open circuit potential in 4.0 mol·L⁻¹ H₂SO₄ with different ILs and equal concentration 15 μg mL⁻¹. Conditions: scan rate, 10 mV s⁻¹; H₂SO₄, 4.0 mol·L⁻¹; immersion time, 5 min.

confirms that E_{corr} decreases in the presence of ILs. It is important to mention that the concentration of ILs on the corrosion of lead-acid batteries affect and going to the best value to 15.0 μg mL⁻¹, because the results of the cyclic voltamograms showed that ILs shift the overpotential of hydrogen evolution to the negative potential, which is decreasing water loss in lead-acid batteries, up to 15.0 μg mL⁻¹.

EIS is a powerful, nondestructive, and informative technique which is usually used for characterization and study of corrosion behaviour. EIS studies on the lead-antimony alloy in 4.0 mol·L⁻¹ H₂SO₄ solutions in the absence and presence

of 15.0 μg mL⁻¹ of the ILs were performed at open circuit corrosion potential. The resulting Nyquist and Bode plots are shown in Figure 7, hence Table 2 shows impedance parameters obtained by the FRA4.9 software for this concentration of ILs. The results showed that the impedance response has significantly changed after the addition of IL on the corrosive solutions. The results explain that charge transfer resistance (R_t) increased by adding of the THAHS, MCHAHS, and BCHAHS, whereas it decreased for HAHS.

The proposed equivalent circuit used to fit the experimental data is shown in Figure 8. R_{el} is the electrolyte

TABLE 1: Corrosion data for Pb 1.6 wt% Sb alloy in 4.0 mol·L⁻¹ H₂SO₄ in presence and absence of ionic liquids obtained from Tafel polarization and electrochemical impedance spectroscopy methods.

Sample	Concentration of IL ($\mu\text{g cm}^{-3}$)	Tafel measurements				EIS measurements	
		E_{corr} (mV)	i_{corr} ($\mu\text{A cm}^{-2}$) Error ($\pm 2-4\%$)	C.R. (mpy) Error ($\pm 2-4\%$)	IE%	R_t (Ω)	IE%
Without IL		-597	14.42	27165.66		178.7	
HAHS	5	-596	10.03	18877.56	30.50		
	10	-589	14.46	27213.94	0.22		
	15	-589	16.16	30432.62	12.03	133.9	33.45
	20	-594	17.57	33104.13	21.80		
MCHAHS	5	-589	9.87	18587.88	31.54		
	10	-593	9.36	17638.37	35.11		
	15	-594	12.53	20808.77	13.14	281.3	36.47
	20	-589	11.05	23609.03	23.40		
THAHS	5	-584	7.27	13695.49	49.60		
	10	-588	9.99	18829.28	30.68		
	15	-594	13.75	25910.37	4.68	240.1	25.57
	20	-596	12.28	23126.22	14.87		
BCHAHS	5	-584	7.29	13727.67	49.46		
	10	-588	6.78	12778.16	52.97		
	15	-594	6.03	11345.85	58.18	307.4	58.13
	20	-596	6.42	12086.15	55.51		

TABLE 2: Impedance parameters obtained by the FRA4.9 software. Simulated results for as-cast Pb 1.6 wt% Sb alloy in a 4.0 M H₂SO₄ solution with and without 15 $\mu\text{g}\cdot\text{L}^{-1}$ ILs at 25°C.

Parameters	Without IL	15 $\mu\text{g}\cdot\text{L}^{-1}$ HAHS	15 $\mu\text{g}\cdot\text{L}^{-1}$ THAHS	15 $\mu\text{g}\cdot\text{L}^{-1}$ MCHAHS	15 $\mu\text{g}\cdot\text{L}^{-1}$ BCHAHS
R_{el} ($\Omega\cdot\text{cm}^{-2}$)	1.443 (± 0.02)	1.418 (± 0.02)	1.447 (± 0.03)	1.400 (± 0.03)	1.410 (± 0.02)
Q_1 ($\text{mF}\cdot\text{cm}^{-2}$)	2.056 (± 0.09)	2.058 (± 0.09)	6.338 (± 0.21)	5.002 (± 0.22)	4.800 (± 0.17)
N	0.8759 (± 0.005)	0.8617 (± 0.005)	0.8470 (± 0.005)	0.8392 (± 0.005)	0.8307 (± 0.005)
R_t ($\Omega\cdot\text{cm}^{-2}$)	178.7 (± 4)	133.9 (± 3)	204.1 (± 4)	281.3 (± 7)	307.4 (± 8)
W ($\pm 5\%$)	0.0313	0.0497	0.0392	0.0283	0.0265

resistance, Q_1 denotes the capacitance of the double layer, R_t is the charge transfer resistance (corrosion resistance), and W is the Warburg impedance.

The impedance measured in the case of the short immersion time (5 min) exhibited Warburg impedance, which is indicating the corrosion process involved in the transport of reactants from the bulk solution to the lead-antimony/solution interface or transport of soluble corrosion products from the interface to the bulk solution in the early stage of corrosion. As mentioned above, the appearance of the Warburg impedance at the corrosion potential in aerated sulfuric acid should be attributed to oxygen transport from the bulk solution to the lead-antimony surface.

Impedance measurements were used to calculate the inhibition efficiency, using $\text{IE}\% = (1 - (R_1^0/R_1)) \times 100$, where R_1 and R_1^0 are the corrosion resistance in the presence and absence of IL in solutions, respectively. As shown in Table 1, it can be observed that the corrosion resistance (R_1) in solutions containing MCHAHS, BCHAHS, and THAHS are higher than in a solution without IL. The results have a good

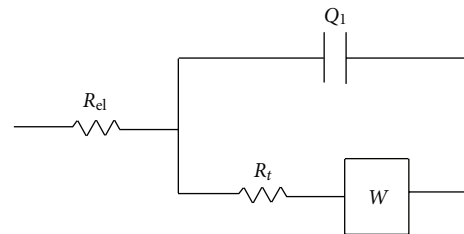


FIGURE 8: Proposed equivalent circuit used for fitting of the impedance spectra.

agreement with the results of the potentiodynamic polarization experiments. It seems that the morphological changes of the PbSO₄ layer which regulate H⁺ ions transportation through different layers play an important role to dictate the corrosion behaviour of the electrode in the presence of IL.

The surface morphology of the lead alloy after one cycle of charge and discharge in sulfuric acid solution in the absence and presence of THAHS was obtained to study PbSO₄ layer morphology (Figure 9). The SEM images confirm that

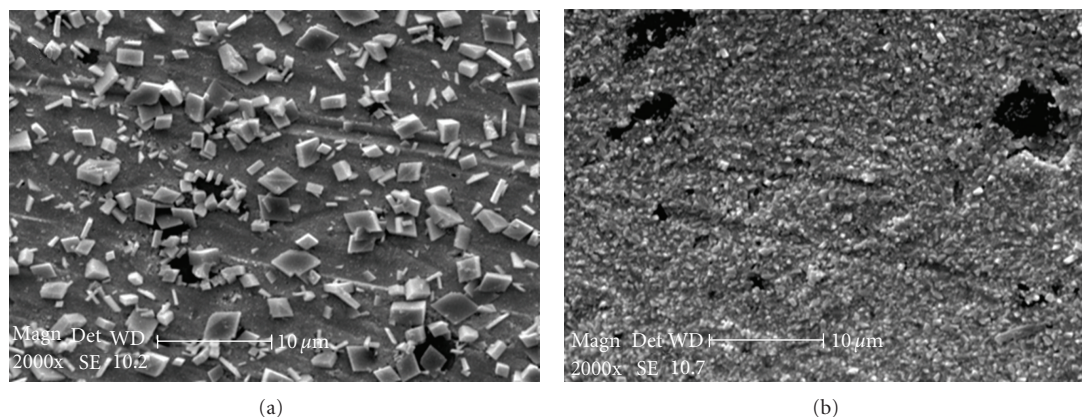


FIGURE 9: The scanning electron micrographs (SEM) of Pb-1.66% Sb-Sn alloy after one cycle of charge and discharge in H_2SO_4 without additive (a) and in the presence of $15.0 \mu\text{g}\cdot\text{L}^{-1}$ of THAHS (b).

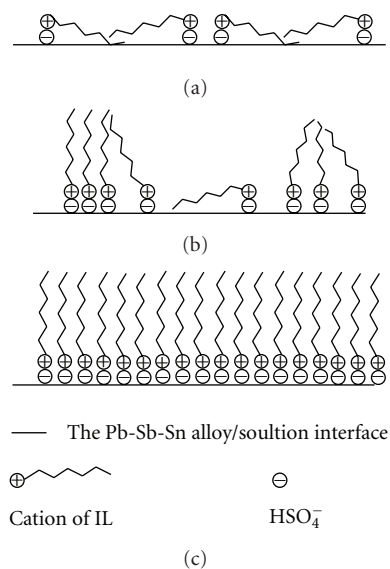


FIGURE 10: Illustration of adsorption of ILs at lead-antimony/solution interface at constant immersion time (5 min). (a) Adsorption as single ILs; (b) hemimicelle formation at some sites of the surface; (c) hemimicelle formation is complete.

smaller and fewer amounts of PbSO_4 are formed on the electrode in the presence of THAHS. It seems that cationic species interact with electrode surface and charged species in the electrolyte and, hence, change the structures of basic lead sulfate formed on the electrode surface. It seems that these cations make it difficult for lead and sulphate ions to form lead sulphate crystals and, subsequently, prevent the growth of existing lead sulphate crystals.

3.3. The Adsorption Model of ILs on the Lead Surface. The inhibitive action of ILs in sulfuric acid solution results from physical (electrostatic) adsorption of the negative charge of RNSO_4^- ($R = 1$ to 4, branch of alkyl or cycloalkyl) to the positive charge (lead surface), forming a barrier on the lead surface.

On the basis of Ma et al.'s model for the adsorption of surfactants on the copper surface [27], IE should decrease

continuously with the immersion time. Thus, the quaternary ammonium cations, $\text{C}_{16}\text{H}_{33}\text{N}(\text{CH}_3)_3$ ions, can be electrostatically adsorbed on the electrode surface covered with primarily adsorbed anion ions. The experimental results were similar to our set of ILs, and the inhibition action of ILs decreased with further increasing in the concentration of ILs in constant time.

By immersing lead antimony alloy in the solution at the constant time (5 min), the orientation of adsorbed ILs on the surface of the electrode greatly affects its inhibitory efficiency. It may be due to the chemisorptions of RN^+ ions and also its electrostatic attraction on the lead surface which can take place (Figure 10(a)). This adsorption has an appropriate free energy change to transferring hydrocarbon chains from water (as a polar media) to the surface. It means that much area can be covered with each adsorbed RN^+ ions thereby inhibiting corrosion efficiency increased. While, by increasing adsorbed RN^+ ions at the electrode surface in higher ILs concentration, the adsorption density of ILs becomes so high. Consequently, the van der Waals interaction between organic tails of RN^+ can occur to form hemimicelle (Figure 10(b)). This behaviour could be observed in the near concentration of $10.0 \mu\text{g mL}^{-1}$ for HAHS, MCHAHS, and THAHS and also in the concentration of $20.0 \mu\text{g mL}^{-1}$ for BCHAHS. This will decrease, the effective covering of electrode surface and so decrease the inhibiting corrosion efficiency. By using higher ILs concentration, the corrosion resistance decreased during surface coverage of all electrode area (Figure 10(c)). After this point corrosion resistance will increase due to formation of second layer by merging of the hydrocarbon chains of ILs. It can create a double layer which increases the corrosion resistance.

4. Conclusion

The corrosion rate of lead-antimony alloy, as a most common using alloy to grid production for lead-acid batteries, is one of the main problems in these industries. Due to this problem, the electrical conductivity of positive and negative plates and straps as an electrical connector decreased during

the time and so decreased battery life time. Therefore, increasing IE by using suitable additives can increase battery life time. In present work, hydrogen, oxygen evolution, and the corrosion behaviour of lead-antimony alloy, in the electrolyte solution of H_2SO_4 $4.0 \text{ mol}\cdot\text{L}^{-1}$, in the presence of four ILs including HAHS, THAHS, MCHAHS, and BCHAHS (consist of alkyl and cycloalkyl ammonium hydrogen sulphate), were studied in various concentrations. All studied ILs increased hydrogen evolution overpotential. Investigation on a family of alkyl ammonium hydrogen sulphate ionic liquids shows that electrochemical behaviour of lead alloy are mainly under the influence of the number of alkyl and cycloalkyl branches in alkyl ammonium cations. Hydrogen evolution potential has a reversed linear correlation with the number of alkyl and cycloalkyl chain. The results show that, in the presence of all studied ILs, fewer and smaller PbSO_4 crystals are formed on the electrode surface. Morphological changes of the PbSO_4 layer play an important role in dictating the electrochemical reactions of lead alloy.

The results show three different ways of behaviours based on ILs concentration; firstly IE increases in the presence of all ILs (at constant immersing time of lead alloy in solution), then decreases by increasing the concentrations of ILs, and finally IE increases again in the presence of excess amounts of ILs. Therefore, the ILs concentration and configuration can be affected by the corrosion behaviour of lead-antimony electrodes. Also, a new adsorption model for ILs on the electrode surface was proposed. Lead surface in sulphuric acid produced lead sulphate, PbSO_4 ; therefore cations of ILs are adsorbed at the surface of lead alloy. The cation of ILs may be adsorbed at the lead surface through both chemisorption and electrostatic attraction. Increasing of ILs concentration at the surface of the electrode has a great influence on the IE of lead-antimony alloy. Also, the corrosion potential (E_{corr}) has been shifted to the positive region in the presence of all kinds of ILs. Finally, the results confirm that the cyclohexylform of ILs in comparison to hexyl form has a lower corrosion rate and higher inhibition efficiency.

Acknowledgment

The authors acknowledge the Isfahan University of Technology Research Council and Center of Excellence in Sensor and Green Chemistry for supporting this work.

References

- [1] D. A. J. Rand, P. T. Moseley, J. Garche, and C. D. Parker, *Valve-Regulated Lead-Acid Batteries*, Elsevier, Amsterdam, Netherlands, 2004.
- [2] L. C. Peixoto, W. R. Osório, and A. Garcia, "The interrelation between mechanical properties, corrosion resistance and microstructure of Pb-Sn casting alloys for lead-acid battery components," *Journal of Power Sources*, vol. 195, no. 2, pp. 621–630, 2010.
- [3] R. D. Prengaman, "Challenges from corrosion-resistant grid alloys in lead acid battery manufacturing," *Journal of Power Sources*, vol. 95, no. 1-2, pp. 224–233, 2001.
- [4] B. Rezaei, M. Taki, and S. Mallakpour, "Application of ionic liquids as an electrolyte additive on the electrochemical behavior of lead acid battery," *Journal of Power Sources*, vol. 187, no. 2, pp. 605–612, 2009.
- [5] B. Rezaei, E. Havakeshian, and A. R. Hajipour, "Influence of acidic ionic liquids as an electrolyte additive on the electrochemical and corrosion behaviors of lead-acid battery," *Journal of Solid State Electrochemistry*, vol. 15, pp. 421–430, 2011.
- [6] P. Delahay, M. Pourbaix, and P. V. Rysseberghe, "Potential-pH diagram of lead and its applications to the study of lead corrosion and to the lead storage battery," *Journal of The Electrochemical Society*, vol. 98, pp. 57–64, 1951.
- [7] W. H. Boctor, S. Zhong, H. K. Liu, and S. X. Dou, "An electrochromic method for evaluation of the corrosion of lead alloys," *Journal of Power Sources*, vol. 77, no. 1, pp. 56–63, 1999.
- [8] J. Garche, "Corrosion of lead and lead alloys: influence of the active mass and of the polarization conditions," *Journal of Power Sources*, vol. 53, no. 1, pp. 85–92, 1995.
- [9] L. T. Lam, T. D. Huynh, N. P. Haigh et al., "Influence of bismuth on the age-hardening and corrosion behaviour of low-antimony lead alloys in lead/acid battery systems," *Journal of Power Sources*, vol. 53, no. 1, pp. 63–74, 1995.
- [10] D. A. J. Rand, "Publications on lead/acid batteries and related phenomena: 10-year compilation 1984–1994," *Journal of Power Sources*, vol. 60, pp. 1–124, 1996.
- [11] S. Zhong, J. Wang, H. K. Liu, S. X. Dou, and M. Skyllas-Kazacos, "Influence of alloying with bismuth on electrochemical behaviour of lead-calcium-tin grid alloys," *Journal of Power Sources*, vol. 66, no. 1-2, pp. 107–113, 1997.
- [12] D. Slavkov, B. S. Haran, B. N. Popov, and F. Fleming, "Effect of Sn and Ca doping on the corrosion of Pb anodes in lead acid batteries," *Journal of Power Sources*, vol. 112, no. 1, pp. 199–208, 2002.
- [13] S. Brinić, M. Metkoš-Huković, and R. Babić, "Impedance spectroscopy as a tool for characterization of surface films on lead and lead alloys," *Journal of New Materials for Electrochemical Systems*, vol. 8, no. 4, pp. 273–282, 2005.
- [14] M. Taguchi, T. Hirasawa, and K. Wada, "Corrosion behavior of Pb-Sn and Pb-2 mass% Sn-Sr alloys during repetitive current application," *Journal of Power Sources*, vol. 158, no. 2, pp. 1456–1462, 2006.
- [15] W. R. Osório, L. C. Peixoto, and A. Garcia, "Electrochemical corrosion of Pb-1 wt% Sn and Pb-2.5 wt% Sn alloys for lead-acid battery applications," *Journal of Power Sources*, vol. 194, no. 2, pp. 1120–1127, 2009.
- [16] A. A. Aksüt and S. Bilgiç, "The effect of amino acids on the corrosion of nickel in H_2SO_4 ," *Corrosion Science*, vol. 33, no. 3, pp. 379–387, 1992.
- [17] G. K. Gomma and M. H. Wahdan, "Effect of temperature on the acidic dissolution of copper in the presence of amino acids," *Materials Chemistry and Physics*, vol. 39, no. 2, pp. 142–148, 1994.
- [18] J. B. Matos, L. P. Pereira, S. M. L. Agostinho, O. E. Barcia, G. G. O. Cordeiro, and E. D. Elia, "Effect of cysteine on the anodic dissolution of copper in sulfuric acid medium," *Journal of Electroanalytical Chemistry*, vol. 570, no. 1, pp. 91–94, 2004.
- [19] W. A. Badawy, K. M. Ismail, and A. M. Fathi, "Corrosion control of Cu-Ni alloys in neutral chloride solutions by amino acids," *Electrochimica Acta*, vol. 51, no. 20, pp. 4182–4189, 2006.
- [20] Z. Ghasemi and A. Tizpar, "The inhibition effect of some amino acids towards Pb-Sb-Se-As alloy corrosion in sulfuric

- acid solution,” *Applied Surface Science*, vol. 252, no. 10, pp. 3667–3672, 2006.
- [21] M. A. Kiani, M. F. Mousavi, S. Ghasemi, M. Shamsipur, and S. H. Kazemi, “Inhibitory effect of some amino acids on corrosion of Pb-Ca-Sn alloy in sulfuric acid solution,” *Corrosion Science*, vol. 50, no. 4, pp. 1035–1045, 2008.
- [22] D. Pavlov, V. Naidenov, and S. Ruevski, “Influence of H₂SO₄ concentration on lead-acid battery performance. H-type and P-type batteries,” *Journal of Power Sources*, vol. 161, no. 1, pp. 658–665, 2006.
- [23] A. R. Hajipour, G. Azizi, and A. E. Ruoho, “Iodination of alcohols under microwave irradiation using KI in the presence of a catalytic amount of ionic liquid triethylammonium hydrogensulfate([Et₃NH]⁺HSO₄⁻),” *Synthetic Communications*, vol. 39, no. 2, pp. 242–250, 2009.
- [24] B. Culpin and D. A. J. Rand, “Failure modes of lead/acid batteries,” *Journal of Power Sources*, vol. 36, no. 4, pp. 415–438, 1991.
- [25] D. Pavlov, M. Bojinov, T. Laitinen, and G. Sundholm, “Electrochemical behaviour of the antimony electrode in sulphuric acid solutions-II. Formation and properties of the primary anodic layer,” *Electrochimica Acta*, vol. 36, no. 14, pp. 2087–2092, 1991.
- [26] D. Pavlov, M. Bojinov, T. Laitinen, and G. Sundholm, “Electrochemical behaviour of the antimony electrode in sulphuric acid solutions-I. Corrosion processes and anodic dissolution of antimony,” *Electrochimica Acta*, vol. 36, no. 14, pp. 2081–2086, 1991.
- [27] H. Ma, S. Chen, B. Yin, S. Zhao, and X. Liu, “Impedance spectroscopic study of corrosion inhibition of Cu by surfactants in the acidic solutions,” *Corrosion Science*, vol. 45, pp. 867–882, 2003.



Hindawi

Submit your manuscripts at
<http://www.hindawi.com>

